Article

Influence of Humidity and Heating Rate on the Continuous ZIF Coating during Hydrothermal Growth

Eunji Choi , Choong Hoo Lee , Dae Woo Kim [*]

Article

Influence of Humidity and Heating Rate on the Continuous ZIF Coating during Hydrothermal Growth

Eunji Choi, Choong Hoo Lee and Dae Woo Kim *

Department of Chemical and Biomolecular Engineering, Yonsei University, Yonsei-ro 50, Seodaemun-gu, Seoul 03722, Republic of Korea

*   Correspondence: audw1105@yonsei.ac.kr

Abstract: Zeolitic imidazolate frameworks (ZIFs) have potential for various gas and ion separations due to their well-defined pore structure and relatively easy fabrication process compared to other metal-organic frameworks. As a result, many reports have focused on preparing polycrystalline and continuous ZIF layers on porous supports. In this study, we investigated how humidity and chamber temperature influence the structure of a ZIF-8 layer prepared by the hydrothermal method. We controlled the chamber temperature (ranging from 50 °C to 70 °C) and relative humidity (ranging from 20 % to 100 %) using a thermos-hygrostat chamber. We found that as the chamber temperature increased, ZIF-8 preferentially grew into particles rather than forming a continuous polycrystalline layer. By measuring the temperature of the reacting solution based on chamber humidity, we discovered that the heating rate of the reacting solution varied with humidity, even at the same chamber temperature. At higher humidity, thermal energy transfer was accelerated as water vapor delivered more energy to the reacting solution. Therefore, a continuous ZIF-8 layer could be formed more easily at low humidity ranges (ranging from 20 % to 40 %), while micron ZIF-8 particles were synthesized at a high heating rate. Our findings suggest that controlling the heating rate of the reacting solution is critical to preparing a continuous ZIF-8 layer, particularly for future scale-up of ZIF-8 membranes.

Keywords: zeolitic imidazolate framework; membrane; nucleation; relative humidity; solution heating rate

1. Introduction

Metal-organic frameworks (MOFs) are a promising class of porous materials for separation applications, such as adsorbents and membranes, due to their well-defined crystalline pore structure [1–3]. Compared to other porous nanomaterials like zeolites, MOFs can be fabricated into membranes using a relatively mild fabrication process without additional pore activation [4,5]. Among the subclasses of MOFs, the zeolitic imidazolate framework (ZIF) has received widespread attention because ZIF has a similar topology to zeolites with tetrahedral transition metal ions linked to imidazole-based ligands [6]. In particular, ZIF-8, which is constructed from Zn^{2+} and 2-methylimidazole, is the most extensively studied ZIF material because its aperture size is suitable for hydrocarbon separation and hydrogen extraction and the aperture size can be easily tuned by ligand exchange or nanomaterial hybridization [7–10]. Therefore, significant efforts have been made to fabricate continuous ZIF-8 membranes such as *in-situ* synthesis (hydrothermal or solvothermal), contra-diffusion synthesis, epitaxial synthesis, oxide conversion, electrochemical deposition, and fluid processing [11–17].

Among the aforementioned preparation methods, *in-situ* synthesis (hydrothermal or solvothermal) is one of the common methods used for the synthesis of ZIF membranes due to its simplicity, scalability, and reproducibility [18–21]. In this method, a mixture of precursor solutions

doi:10.20944/preprints202303.0152.v1

2

containing metal ions and organic ligands is placed in a bottle and heated at elevated temperatures in the presence of water or other solvents. The resulting conditions create an environment that promotes the formation and growth of ZIF crystals on a porous substrate, which serves as the support for the ZIF membrane [21]. When the nucleated crystals are merged into a polycrystalline layer, membrane fabrication is achieved. However, even if the fabrication process is simple, the quality of the grown ZIF is highly sensitive to growth conditions, and the presence of small defects results in poor gas separation performance.

Previous research has identified several factors that affect the microstructure and quality of synthesized ZIF-8 membranes, such as the nature of the zinc precursors (e.g., zinc nitrate, chloride, and acetate), solvent types (including polarity and precursor-solvent interactions), concentrations and molar ratio of metal ion/organic ligands [22–26]. In addition to these factors, we investigated the effect of relative humidity and chamber temperature on the structure of ZIF-8 layers formed during hydrothermal growth. We used a thermo-hygrostat chamber to control the temperature and relative humidity while conducting hydrothermal growth of ZIF-8 for one hour, recording the heating rate of the reacting solutions. We analyzed the morphology, crystallinity, and size distribution of the synthesized ZIF-8 particles under various reaction temperatures and relative humidity conditions.

2. Materials and Methods

2.1. Materials

Zinc nitrate hexahydrate (Zn(NO$_3$)·6H$_2$O, 98 %, Sigma-Aldrich) and 2-methylimidazole (2-MIM, 99.0 %, Sigma-Aldrich) were used as the metal and ligand sources. Glass substrate (Duran, 18 * 18 mm) was used for ZIF-8 growth. All the chemicals and materials were used as purchased without further purification.

2.2. Synthesis of ZIF-8 Layer with Different Humidity and Temperature

To synthesize a ZIF-8 layer, zinc nitrate hexahydrate (5.5 g) and 2-MIM (105.5 g) were dissolved separately in 1 L of DI water to obtain zinc ion and 2-MIM solutions, respectively. Then, 100 mL of each solution was mixed at room temperature in a molar ratio of 1:45, which has been widely reported as optimal for continuous ZIF membrane growth [7,8]. We like to note that solvent can change the growth kinetics and morphology of ZIF particles, therefore, only water was used for this study. The mixed solution was placed in a thermo-hygrostat chamber as shown in **Scheme 1**, where temperature and relative humidity were precisely controlled. The temperature of the precursor solution was measured using a thermometer. The glass substrate was then immersed in the solution for 1 hour to allow ZIF-8 growth. Afterward, the substrate was immersed in DI water to remove any unreacted precursors and overgrown ZIF-8 particles.
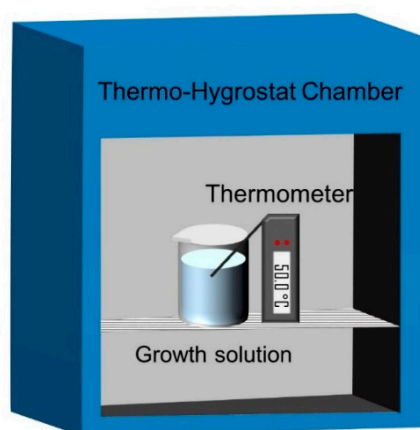
Scheme 1. Schematic for the experiment set-up for ZIF-8 growth.

2.3. Characterization

The morphology of ZIF-8 crystal was observed using scanning electron microscopy (SEM, 7610F-PLUS, JEOL) and x-ray diffraction (XRD) patterns by a film XRD system (Ultima IV, Rigaku, 3 kW sealed Cu Kα X-ray source, λ = 1.5406 Å). Fourier Transform Infrared Spectroscopy (FT-IR, ALPHA II, USA, Bruker) was used to determine the chemical bonding of the ZIF-8 films or particles.

3. Results and Discussions

3.1. Morphology of ZIF-8 Crystal Depending on Chamber Temperature and Relative Humidity

The hydrothermal method is widely used to synthesize ZIF-8 membranes due to its ability to provide controlled growth conditions, resulting in high-quality crystals. It is a scalable and reproducible method that is relatively simple and cost-effective compared to other methods. ZIF-8 membranes with excellent separation performance have been reported using the hydrothermal method [7,8]. In this study, we focused on the growth of ZIF-8 and the effect of growth conditions, specifically the relative humidity and temperature of the chamber, while keeping other growth conditions identical. Water was used as a solvent to avoid the solvent effect on the nucleation and growth of ZIF-8. We used a cover glass substrate for ZIF-8 growth, which was chosen for its simplicity and convenience in the ZIF-8 fabrication, as well as its similar chemical structure to conventional ceramic substrates such as alumina and silica with oxygen groups [27]. Firstly, ZIF-8 growth on a glass substrate was observed at 50 °C by varying the relative humidity from 20 % to 100 %, and the morphology and crystal structure were investigated (**Figure 1**). Our results showed that ZIF-8 films were continuous and highly crystalline at relative humidities between 20 % and 40 % (**Figure 1a–c**). However, at higher relative humidities, ZIF-8 crystals formed as island particles rather than a continuous film (**Figure 1d–f**). Notably, we observed large and highly crystalline ZIF-8 particles at 60 % relative humidity, while small ZIF-8 particles were present above 80 % relative humidity.
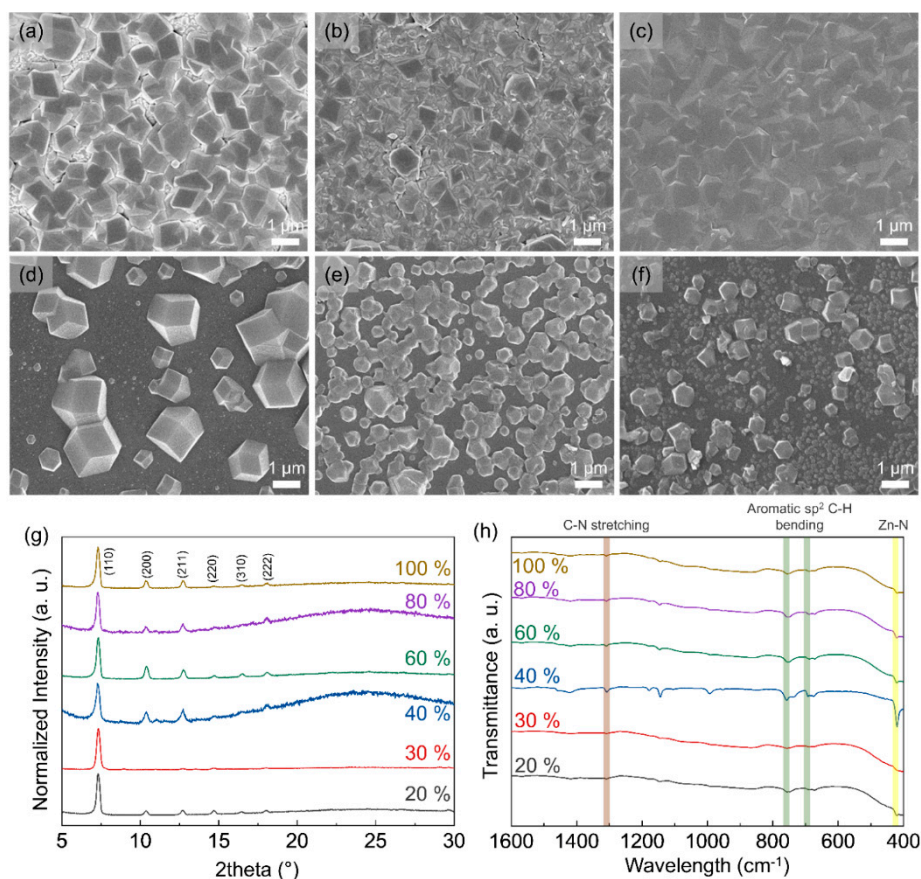

Figure 1. (**a-f**) SEM images, (**g**) XRD patterns and (**h**) FT-IR spectra of ZIF-8 crystals depending on relative humidity (20, 30, 40, 60, 80, and 100 %). The temperature of the chamber was 50 °C.

The crystal structure of ZIF-8 layer or particles was investigated using XRD, showing the major XRD six peaks of ZIF-8 within 20 degrees without clear differences (**Figure 1g**). The FT-IR investigation of ZIF-8 film or particles was also performed. ZIF-8 peaks, such as the stretching vibration of Zn-N bond at 426 cm^{-1}, the aromatic sp^2 bending of 2-MIM at 678 and 737 cm^{-1}, and the stretching C-N bond at 1310 cm^{-1}, were observed [28]. These results indicate that the morphology of grown ZIF-8 is highly influenced by the relative humidity of the chamber while other conditions were identical. However, their crystalline structure with various relative humidity were identical at 50 °C of the chamber temperature.

In order to investigate the effect of temperature and relative humidity during the ZIF-8 growth, the chamber temperature was increased from 50 °C to 60 °C with relative humidities ranging from 20 % to 40 % (**Figure 2**). Continuous ZIF-8 layers were not formed at 60 °C, with particle size varying depending on the relative humidity of the chamber. At 60 °C and 20 % humidity, ZIF-8 particle size was around 400 - 500 nm (**Figure 2a**). Increasing the relative humidity led to a significant increase in particle size, up to 1 μm (**Figure 2b,c**). Unlike ZIF-8 particles with high relative humidity at 50 °C, these ZIF-8 particles at 60 °C exhibited high crystallinity and chemical bonding with distinct facets of ZIF-8, possibly due to their large size (**Figure 2d,e**). It is known that deprotonation of 2-MIM can be facilitated at higher temperatures [29], leading to more nucleation of ZIF-8 seeds. However, the growth of relatively larger ZIF-8 particles at higher temperatures can be attributed to more facilitated particle growth than nucleation.
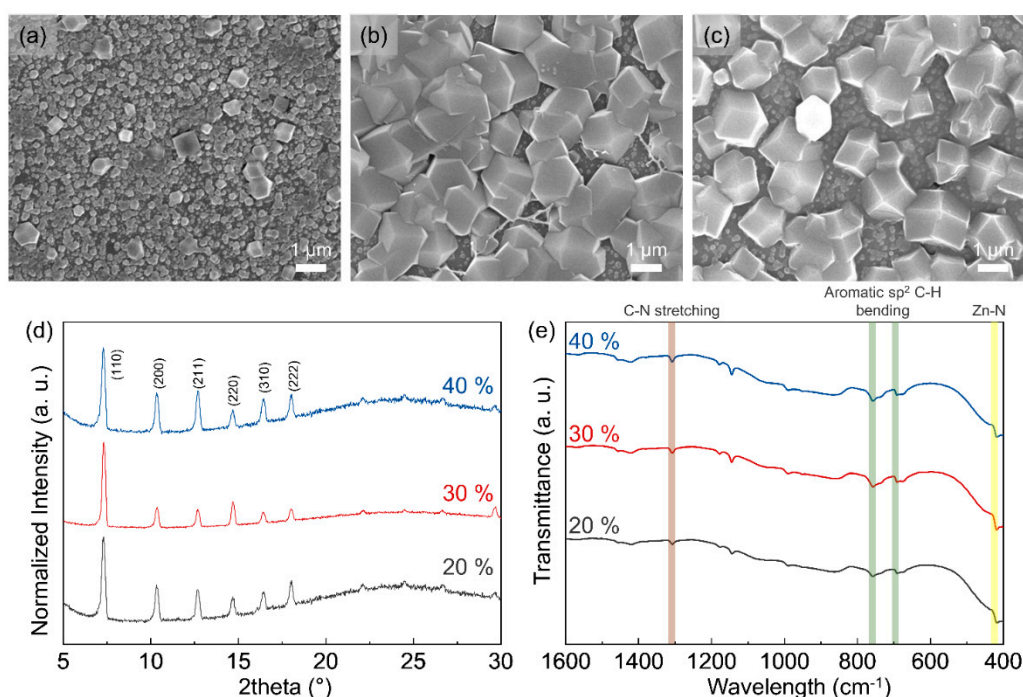

Figure 2. (**a-c**) SEM images, (**d**) XRD patterns and (**e**) FT-IR spectra for the ZIF-8 grown on the substrates depending on relative humidity (20, 30, and 40 %) at chamber temperature of 60 °C.

ZIF-8 particles were synthesized at 70 °C under relative humidity conditions ranging from 20 % to 40 % to investigate their growth at higher temperatures (**Figure 3**). Uniform and micro-sized particles were observed at 20 % relative humidity, as shown in **Figure 3a**. In contrast, ZIF-8 particles synthesized at 30 % and 40 % relative humidity appeared as clusters with low crystallinity, and the grain boundary of the ZIF-8 crystal was not observed clearly in **Figures 3b** and **3c**. Interestingly, the XRD peaks of ZIF-8 particles synthesized at 20 % relative humidity were very sharp with a preferential (110)-orientation. While the reason is not clear at this point, the preferential orientation of ZIF-8 is interesting. Because this study is not focused on crystalline orientation, further study will be reported soon. The diffraction of 2-MIM for the ZIF-8 particles synthesized at 30 % and 40 % was

strongly observed near 18 degrees, indicating the growth of ZIF-8 particles by combining with 2-MIM, as shown in **Figure 3d**. Notably, several FT-IR spectra in **Figure 3e** for ZIF-8 were observed at this temperature and relative humidity, indicating no significant change in the chemical bonding of ZIF-8.
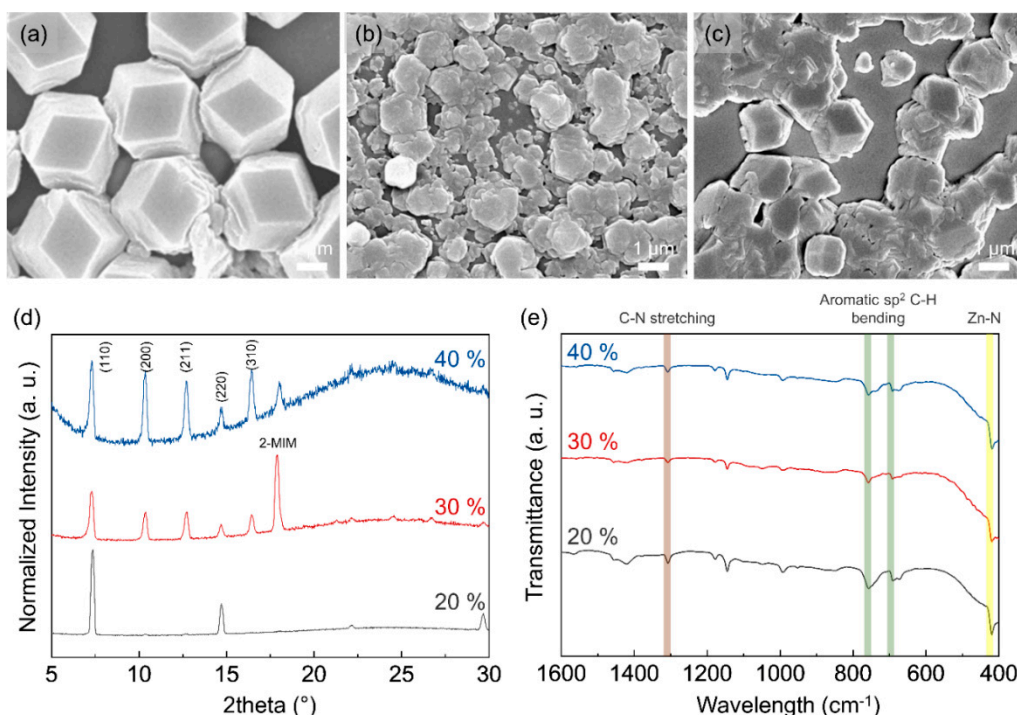

Figure 3. (**a-c**) SEM images, (**d**) XRD patterns and (**e**) FT-IR spectra for the ZIF-8 grown on the substrates depending on relative humidity (20, 30, and 40 %) at chamber temperature of 70 °C.

3.2. Particle and Grain Size Distribution

The effects of different temperature and relative humidity conditions on the size of ZIF-8 grains or particles are summarized in **Figure 4**. For polycrystalline ZIF-8 coating (sky blue area), most of the grain sizes ranged from 500 - 1200 nm, and no significant changes in grain size were observed. However, at a constant temperature of 50 °C, an increase in relative humidity (60 %) led to an increase in the grain size of ZIF-8 particles, reaching several micrometers from nanometers, followed by a dramatic decrease in grain size ranging from 300-700 nm, particularly at 80 % and 100 % relative humidity. Moreover, the particle size of ZIF-8 increased (yellow area) to several micrometers at 60 °C and 70 °C, regardless of the relative humidity. Notably, the ZIF-8 particles at 70 °C consistently had a large particle size of about 3 μm with a highly oriented crystal structure. Since the ZIF-8 layer used for the membrane fabrication is very thin (sub-micrometer thickness), the formation of micrometer-scale particles is not suitable for producing a continuous polycrystalline ZIF-8 layer. Therefore, the importance of optimizing conditions such as temperature and relative humidity might be increased.

To investigate the relationship between relative humidity and the growth mechanism of ZIF-8, the temperature profiles of the growth solution were measured at a chamber temperature of 50 °C for several humidity ranges. The temperature in the reacting solution was measured using a portable thermometer (**Scheme 1**). **Figure 5a** shows that the temperature of all solutions increased in the first 15 minutes and then stabilized, indicating two different heating rate trends. The heating rate depending on the relative humidity was calculated in **Figure 5b**, which was determined from the slope of **Figure 5a**. The heating rate was similar at low humidity (20 – 40 %), ranging from 1 – 2 °C/min, but it dramatically increased at high humidity (60 – 100 %), ranging from 2.5 – 3.5 °C/min.
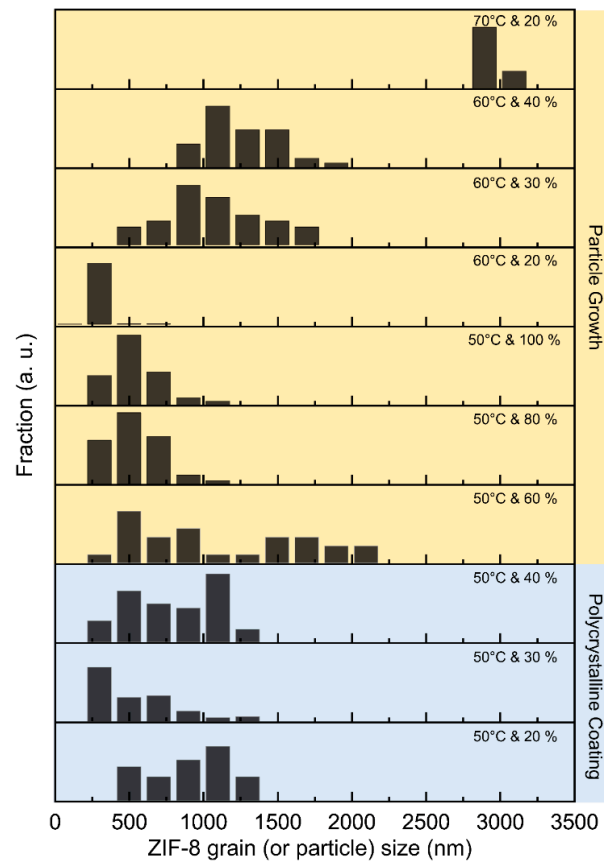
Figure 4. ZIF-8 grain (or particle) size distribution depending on the temperature and relative humidity. Because crystallinity of ZIF-8 was not high at the relative humidity (30 and 40 %) and 70 °C, the grain size was not measured.
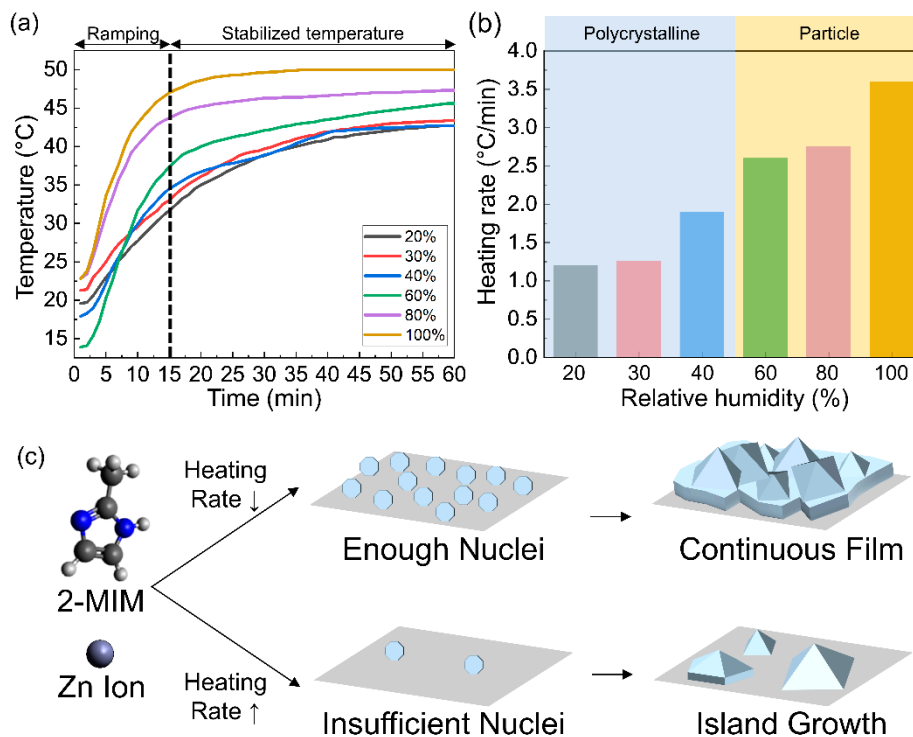

Figure 5. (**a**) Temperature profile and (**b**) the heating rate graphs of the reacting solutions during ZIF-8 growth at 50 °C for different relative humidities. (**c**) A schematic diagram of the growth mechanism of ZIF-8 crystals depending on the heating rate of the reaction solution.

The presence of water vapor in the air can enhance thermal energy transfer due to the increased heat capacity of water molecules compared to dry air. This means that water molecules require more energy to raise their temperature, which can then be transferred to other objects or surfaces through convection or conduction. Therefore, even if the chamber temperature is the same, the real temperature of the reacting solution can significantly differ depending on the number of relative humidity. Due to that, competitive reactions between nucleation and crystal growth of ZIF-8 are occurred in the reacting solution, leading to different growth mechanisms and kinetics. Based on previous studies on ZIF-8 particle growth in solution, sometimes increasing the growth temperature can lead to an increase in the size of ZIF-8 particles because higher temperatures can increase the growth rate of ZIF-8 crystal [29]. On the other hand, high temperature can also facilitate the deprotonation of 2-MIM, which is favorable to form nuclei, leading to small particle size [30,31]. In addition, excessively high temperatures (above 70 °C) may not be suitable for ZIF-8 crystal formation. Therefore, continuous ZIF-8 coating process is highly complicated with various factors.

To summarize, at a fixed temperature of 50 °C, the formation of enough ZIF-8 nuclei resulted in the formation of a polycrystalline film with a uniform grain size of 500 - 1200 nm at low heating rates of the reacting solution. However, at high heating rates (**Figure 5c**), insufficient ZIF-8 nuclei were formed, leading to island growth of ZIF-8 crystals with varying particle sizes. Furthermore, island growth with low crystallinity was also observed at higher temperatures of 60 °C and 70 °C. The precise relationship between growth temperature and particle size can vary depending on other factors such as precursor concentration, solvent, reaction time, and even by substrate [32,33]. Therefore, the critical temperature and relative humidity range suitable for membrane fabrication may differ based on experimental conditions and environmental factors. Nonetheless, our observations highlight the significance of considering chamber temperature and relative humidity, which have not been given much importance previously.

4. Conclusions

We demonstrated that the morphology of ZIF-8 can be dramatically influenced by the relative humidity and temperature of the chamber that is used for hydrothermal synthesis. Generally, the temperature of the chamber is considered as the growth condition, but in reality, the temperature change of the growth solution has a significant impact on the growth of ZIFs rather than the temperature of the chamber. To explore the impact of different parameters on ZIF-8 growth, we employed a well-controlled thermo-hygrostat chamber during the ZIF-8 growth reaction. During the *in-situ* growth of ZIF-8 in this chamber, we observed the ZIF-8 nucleation in the early stages, but the number of ZIF-8 nuclei varied depending on the temperature and relative humidity. As a result, different types of ZIF-8 films or particles formed. In particular, the heating rate of the reacting solutions varied accordingly, therefore, it is highly important to manipulate the heating rate or relative humidity for specific applications. Our study provides the first comprehensive report on the relationship between relative humidity and ZIF-8 growth tendencies. In particular, this phenomenon is crucial for the future manufacturing of large-area membranes. For large-scale synthesis, it is necessary to uniformly control the solvent temperature to ensure a reproducible membrane manufacturing process. Although the observed growth conditions are limited to the hydrothermal process, it implies that humidity and temperature control may also be important in other fabrication methods.

Author Contributions: Conceptualization, D. W. K.; methodology, D. W. K., E. C. and C. H. L.; validation, D. W. K. and E. C.; investigation, D. W. K., E. C. and C. H. L.; data curation, E. C.; writing—original draft preparation, D. W. K., E. C. and C. H. L.; writing—review and editing, D. W. K., E. C. and C. H. L.; visualization, D. W. K. and E. C.; supervision, D. W. K.; project administration, D. W. K.; All authors have read and agreed to the published version of the manuscript.

Conflicts of Interest: The authors declare no conflict of interest.

References

1. Wang, H.; Dong, X.; Colombo, V.; Wang, Q.; Liu, Y.; Liu, W.; Wang, X.L.; Huang, X.Y.; Proserpio, D.M.; Sironi, A.; Han, Y; Li, J.; Tailor-Made Microporous Metal–Organic Frameworks for the Full Separation of Propane from Propylene Through Selective Size Exclusion. *Adv. Mater.* **2018**, *30*, 1805088.
2. Cui, W.G.; Hu, T.L.; Bu, X.H.; Metal–Organic Framework Materials for the Separation and Purification of Light Hydrocarbons. *Adv. Mater.* **2019**, *32*, 1806445.
3. Yuan, S.; Feng, L.; Wang, K.; Pang, J.; Bosch, M.; Lollar, C.; Sun, Y.; Qin, J.; Yang, X.; Zhang, P.; Wang, Q.; Zou, L.; Zhang, Y.; Zhang, L.; Fang, Y.; Li, J.; Zhou, H.-C.; Stable Metal–Organic Frameworks: Design, Synthesis, and Applications. *Adv. Mater.* **2018**, *30*, 1704303.
4. Wang, H.; Liu, Y.; Li, J.; Designer Metal–Organic Frameworks for Size-Exclusion-Based Hydrocarbon Separations: Progress and Challenges. *Adv. Mater.* **2020**, *32*, 2002603.
5. Li, J.; Bhatt, P.M.; Li, J.; Eddaoudi, M.; Liu, Y.; Recent Progress on Microfine Design of Metal–Organic Frameworks: Structure Regulation and Gas Sorption and Separation. *Adv. Mater.* **2020**, *32*, 2002563.
6. Krokidas, P.; Moncho, S.; Brothers, E.N.; Castier, M.; Economou, I.G.; Tailoring the gas separation efficiency of metal organic framework ZIF-8 through metal substitution: a computational study. *Phys. Chem. Chem. Phys.* **2018**, *20*, 4879-4892,
7. Choi, E.; Hong, S.J.; Kim, Y.J.; Choi, S.E.; Choi, Y.; Kim, J.H.; Kang, J.; Kwon, O.; Eum, K.; Han, B.; Kim, D.W.; Pore Tuning of Metal-Organic Framework Membrane Anchored on Graphene-Oxide Nanoribbon. *Adv. Funct. Mater.* **2021**, *31*, 2011146.
8. Choi, E.; Choi, J.I.; Kim, Y.J.; Kim, Y.J.; Eum, K.; Choi, Y.; Kwon, O.; Kim, M.; Choi, W.; Ji, H.; Jang, S.S.; Kim, D.W.; Graphene Nanoribbon Hybridization of Zeolitic Imidazolate Framework Membranes for Intrinsic Molecular Separation. *Angew. Chem. Int. Ed.* **2022**, *61*, e202214269.
9. Fan, W.; Ying, Y.; Peh, S.B.; Yuan, H.; Yang, Z.; Yuan, Y.D.; Shi, D.; Yu, X.; Kang, C.; Zhao, D.; Multivariate Polycrystalline Metal–Organic Framework Membranes for CO_2/CH_4 Separation. *J. Am. Chem. Soc.* **2021**, *143*, 17716-17723.
10. Lee, M.J.; Kwon, H.T.; Jeong, H.K. High-Flux Zeolitic Imidazolate Framework Membranes for Propylene/Propane Separation by Postsynthetic Linker Exchange. *Angew. Chem. Int. Ed.* **2017**, *57*, 156-161.
11. Zhou, Y.; Zhang, X.-F.; Yao, J.; Wang, H.; Contra-diffusion synthesis of metal-organic framework separation membranes: A review. *Sep. Pur. Technol.* **2022**, *300*, 121837.
12. Bux, H.; Liang, F.; Li, Y.; Cravillon, J.; Wiebcke, M.; Caro, J.; Zeolitic imidazolate framework membrane with molecular sieving properties by microwave-assisted solvothermal synthesis. *J. Am. Chem. Soc.* **2009**, *131*, 16000-16001.
13. Yeo, Z.Y.; Zhu, P.W.; Mohamed, A.R.; Chai, S.-P.; A well inter-grown ZIF-8 membrane synthesized via two-step hydrothermal synthesis on coarse α-Al_2O_3 support. *Mater. Lett.* **2014**, *129*, 162-165.
14. Eum, K.; Rownaghi, A.; Choi, D.; Bhave, R.R.; Jones, C.W.; Nair, S.; Fluidic Processing of High-Performance ZIF-8 Membranes on Polymeric Hollow Fibers: Mechanistic Insights and Microstructure Control. *Adv. Funct. Mater.* **2016**, *26*, 5011-5018.
15. Zhao, Y.; Wei, Y.; Lyu, L.; Hou, Q.; Caro, J.; Wang, H.; Flexible Polypropylene-Supported ZIF-8 Membranes for Highly Efficient Propene/Propane Separation. *J. Am. Chem. Soc.* **2020**, *142*, 20915-20919.
16. Neelakanda, P.; Barankova, E.; Peinemann, K.-V.; Polymer supported ZIF-8 membranes by conversion of sputtered zinc oxide layers. *Microporous and Mesoporous Mater.* **2016**, *220*, 215-219.
17. Valadez Sánchez, E.P.; Gliemann, H.; Haas-Santo, K.; Wöll, C.; Dittmeyer, R.; ZIF-8 SURMOF Membranes Synthesized by Au-Assisted Liquid Phase Epitaxy for Application in Gas Separation. *Chem. Ing. Tech.* **2016**, *88*, 1798-1805.
18. Kwon, H.T.; Jeong, H.-K.; In Situ Synthesis of Thin Zeolitic–Imidazolate Framework ZIF-8 Membranes Exhibiting Exceptionally High Propylene/Propane Separation. *J. Am. Chem. Soc.* **2013**, *135*, 10763-10768.
19. Isaeva, V.I.; Barkova, M.I.; Kustov, L.M.; Syrtsova, D.A.; Efimova, E.A.; Teplyakov, V.V.; In situ synthesis of novel ZIF-8 membranes on polymeric and inorganic supports. *J. Mater. Chem. A* **2015**, *3*, 7469-7476.
20. Liu, Y.; Wang, N.; Pan, J.H.; Steinbach, F.; Caro, J.; In situ synthesis of MOF membranes on ZnAl-CO_3 LDH buffer layer-modified substrates. *J. Am. Chem. Soc.* **2014**, *136*, 14353-14356.
21. Shah, M.; Kwon, H.T.; Tran, V.; Sachdeva, S.; Jeong, H.-K.; One step in situ synthesis of supported zeolitic imidazolate framework ZIF-8 membranes: Role of sodium formate. *Microporous and Mesoporous Mater.* **2013**, *165*, 63-69.
22. He, M.; Yao, J.; Li, L.; Zhong, Z.; Chen, F.; Wang, H.; Aqueous solution synthesis of ZIF-8 films on a porous nylon substrate by contra-diffusion method. *Microporous and Mesoporous Mater.* **2013**, *179*, 10-16.

23. Ramu, G.; Lee, M.; Jeong, H.-K.; Effects of zinc salts on the microstructure and performance of zeolitic-imidazolate framework ZIF-8 membranes for propylene/propane separation. *Microporous and Mesoporous Mater.* **2018**, *259*, 155-162.

24. Watanabe, S.; Ohsaki, S.; Hanafusa, T.; Takada, K.; Tanaka, H.; Mae, K.; Miyahara, M.T.; Synthesis of zeolitic imidazolate framework-8 particles of controlled sizes, shapes, and gate adsorption characteristics using a central collision-type microreactor. *Chem. Eng. J.* **2017**, *313*, 724-733.

25. Yao, J.; Li, L.; Benjamin Wong, W.H.; Tan, C.; Dong, D.; Wang, H.; Formation of ZIF-8 membranes and crystals in a diluted aqueous solution. *Mater. Chem. Phys.* **2013**, *139*, 1003-1008.

26. Bustamante, E.L.; Fernández, J.L.; Zamaro, J.M.; Influence of the solvent in the synthesis of zeolitic imidazolate framework-8 (ZIF-8) nanocrystals at room temperature. *J. Colloid Interface Sci.* **2014**, *424*, 37-43.

27. Nagai, N.; Hashimoto, H.; FT-IR-ATR study of depth profile of SiO_2 ultra-thin films. *Applied surface science* **2001**, *172*, 307-311.

28. Tanaka, S; Tanaka, Y; A Simple Step toward Enhancing Hydrothermal Stability of ZIF-8. *ACS Omega* **2019**, *4*, 19905-19912.

29. Saliba, D.; Ammar, M.; Rammal, M.; Al-Ghoul, M.; Hmadeh, M.; Crystal Growth of ZIF-8, ZIF-67, and Their Mixed-Metal Derivatives. *J. Am. Chem. Soc.* **2018**, *140*, 1812-1823.

30. Wu, R.; Fan, T.; Chen, J.; Li, Y.; Synthetic Factors Affecting the Scalable Production of Zeolitic Imidazolate Frameworks. *ACS Sustain. Chem. Eng.* **2019**, *7*, 3632-3646.

31. Xue, Y.; Zhao, Q.; Luan, C.; The Thermodynamic Relations between the Melting Point and the Size of Crystals. *J. Colloid Interface Sci.* **2001**, *243*, 388-390.

32. Choi, E.; Lee, J.; Kim, Y.-J.; Kim, H.; Kim, M.; Hong, J.; Kang, Y. C.; Koo, C. M.; Kim, D. W.; Kim, S. J.; Enhanced Stability of $Ti_3C_2T_x$ MXene Enabled by Continuous ZIF-8 Coating. *Carbon* **2022**, *191*, 593-599.

33. Kwon, O.; Kim, M.; Choi, E.; Bae, J. H.; Yoo, S.; Won, J. C.; Kim, Y. H.; Shin, J. H.; Lee, J. S.; Kim, D. W.; High-aspect Ratio Zeolite Framework (ZIF) Nanoplates for Hydrocarbon Separation Membranes. *Sci. Adv.* **2022**, 8, 1, eabl6841.